PHYSICAL REVIEW E VOLUME 60, NUMBER 1 JULY 1999

Mean discharge frequency locking in the response of a noisy neuron model to subthreshold periodic stimulation

Tetsuya Shimokawa, K. Pakdaman, and Shunsuke Sato
Department of System and Human Science, Graduate School of Engineering Science, Osaka University, Toyonaka 560-8531, Osaka, Japan

(Received 8 February 1999)

Leaky integrate-and-fire neuron models display stochastic resonancelike behavior when stimulated by subthreshold periodic signal and noise. Previous works have shown that matching between the time scales of the noise induced discharges and the modulation period can account for this phenomenon at low modulation amplitudes, but not large subthreshold modulation amplitude. In order to examine the discharge patterns of the model in this regime, we introduce a method for the computation of the power spectral density of the discharge train. Using this method, we clarify the role of the distribution of the input phase at discharge times. Finally, we argue that for large subthreshold inputs, mean discharge frequency locking accounts for the enhanced response. [S1063-651X(99)50207-9]

PACS number(s): 87.10.+e,07.05.Mh

Experimental and theoretical studies have shown the possibility for noise to assist sensory neurons in the detection of weak signals [1], through stochastic resonance (SR). However, whether nervous systems do operate in conditions promiscuous for this phenomenon has not been completely established yet. This question has motivated investigations aiming to clarify conditions under which SR-like behavior occurs in excitable systems and their models [2].

In the conventional form of SR, the response of a particle in a double-well potential to a weak periodic signal becomes maximal when the mean rate of interwell jumps, induced by noise alone, is close to the modulation frequency (for reviews on SR see [3]). This phenomenon is referred to as time-scale matching.

In a similar way, time-scale matching has been proposed as one possible mechanism underlying SR-like behavior in excitable systems [4–7]. The present work shows that, in excitable systems, as in static threshold devices and bistable systems [8], another mechanism, namely, mean discharge frequency locking may be responsible for noise enhanced response to large subthreshold modulations. To this end, we consider the periodically forced noisy leaky integrate-and-fire model (LIFM):

$$dV(t)=\left(-\frac{V(t)}{\tau}+\mu+A\sin(\Omega t+\theta)\right)dt+\sqrt{2D}\,dW(t) \tag{1}$$

for $V(t)<S_0$. If $V(t)=S_0$ then $V(t^+)=V_0<S_0$. In Eq. (1), V represents the membrane potential, τ represents the characteristic membrane charge-discharge time, $\mu\tau$ represents the resting potential, S_0 represents the threshold, and V_0 represents the post-discharge potential. A, $\Omega=2\pi/T$, and θ are, respectively, the input amplitude, angular frequency, and initial phase; D is the noise intensity and $W(t)$ is the standard Wiener process, whose formal derivative is white Gaussian noise. The output of this model consists of the sequence of pulses generated at each discharge.

Periodic forcings are classified as endogenous and exogenous depending on whether the phase of the signal is reset to some fixed value after each firing or not [9]. For endogenous forcing, the spike train forms a renewal process because interspike intervals (ISIs) are independent and identically distributed random variables. Therefore, the power spectral density (PSD) of the spike train is given by [4,10,7]:

$$P_r(\omega)=\frac{1}{\pi\langle t\rangle}\left(1+\frac{\tilde{i}(\omega)}{1-\tilde{i}(\omega)}+\frac{\tilde{i}(-\omega)}{1-\tilde{i}(-\omega)}\right), \tag{2}$$

where i is the ISI distribution, $\langle t\rangle=\int_0^\infty t\;\; i(t)dt$ is the mean ISI, and

$$\tilde{i}(\omega)=\int_0^\infty i(t)\exp[j\omega t]dt. \tag{3}$$

The signal to noise ratio (SNR), denoted by S^1, is then given by [10,7]

$$S^1=\pi\langle t\rangle\max\{P_r(\omega)\;\; :0.93\leqslant\omega\leqslant 1.07\;\;\Omega\}. \tag{4}$$

It has been shown that the LIFM with endogenous forcing displays SR-like behavior in the sense that S^1 goes through a maximum as the noise is increased [10]. However, a systematic investigation of the effect of signal amplitude revealed that, for large subthreshold modulation, the optimal noise level does not correspond to the value predicted by time-scale matching [7]. For instance, for the parameters in [10], S^1 is maximal at $D\simeq 2.5\times 10^{-6}$ $[(\mathrm{mV})^2/(\mathrm{ms})]$ (upper panel Fig. 1), whereas, in the absence of modulation, the mean ISI equals T for a noise intensity $D\simeq 1.9\times 10^{-4}$ $[(\mathrm{mV})^2/(\mathrm{ms})]$. The discrepancy between these values indicates that time-scale matching does not account for the enhanced response of the system.

In order to elucidate the mechanisms underlying this effect of noise, we examine two issues: (i) whether a similar phenomenon occurs for exogenous forcing and (ii) whether a mechanism other than time-scale matching can account for the SR-like behavior in this model.

The first issue is related to the fact that for suprathreshold forcing the phase of the input at the discharge time (hence-

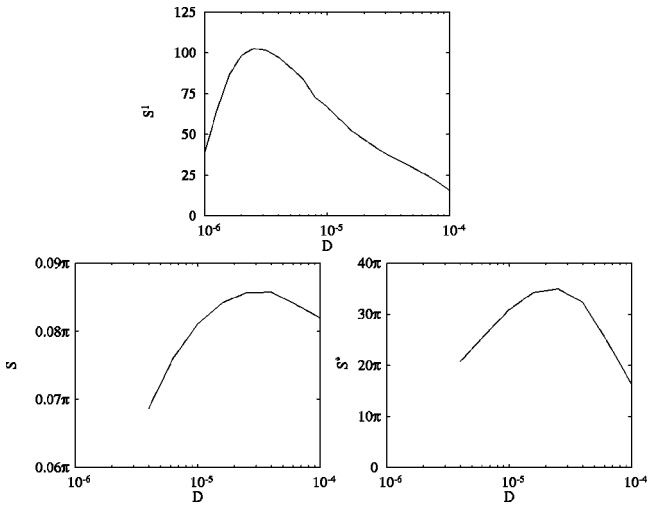

FIG. 1. SNR for endogenous (upper panel) and exogenous (lower panels) forcings. All three ordinates are dimensionless, while all three abscissae represent noise intensity in $[(\mathrm{mV})^2/(\mathrm{ms})]$. Parameters: $S_0=1$ mV, $T=20$ ms, $\tau=1$ ms, $\mu=0.97$ V/s, and $A=0.03$ V/s.

forth referred to as the discharge phase) plays a prominent role in determining the response of the system [11]. Therefore, for large subthreshold signals, it could also strongly influence discharge train characteristics. However, at this stage, the studies of the response of the LIFM in the frequency domain have mainly dealt with the endogenous forcing. In the case of exogenous forcing, the pulse train emitted by the model no longer forms a renewal process, so that neither the PSD nor the SNR can be evaluated by Eqs. (2) and (4). The first part of this paper is devoted to the development of a method for the computation of these quantities for the exogenously forced LIFM. The approach presented here extends the analysis performed in the time-domain in [7], which takes into account the distribution of the input phase at discharge times (henceforth referred to as the phase distribution).

Power spectral density of exogenously forced LIFM. Assuming that the LIFM fires at a phase θ, we denote by $g(t|\theta)$ the distribution of the next ISI. The conditional density g corresponds to the probability density function of the first-passage time of an Ornstein-Uhlenbeck process through a suitable boundary, and can be evaluated numerically as the solution of an integral equation. In [7], the phase distribution h and the ISI distribution i were derived from g for the time domain analysis. For the frequency domain, we show that the autocorrelation and the PSD of the spike train can also be computed from the conditional densities g and the phase distribution h.

More precisely, assuming that a reference discharge occurs at a phase θ, we denote by $l(t|\theta)dt$ the probability to have a discharge in the following interval $(t,t+dt)$. We have

$$l(t|\theta)=\sum_{n=1}^{\infty} l_n(t|\theta), \tag{5}$$

where $l_n(t|\theta)dt$ is the probability for the nth discharge following the reference event to be in the interval $(t,t+dt)$. Thus $l_1(t|\theta)=g(t|\theta)$, and for $n\geqslant 2$ we have

$$l_n(t|\theta)=\int_0^t g(t-u|[\theta+\Omega u])l_{n-1}(u|\theta)du, \tag{6}$$

where the square brackets in $[\theta+\Omega u]$ indicate that this quantity is taken modulo 2π. Using the phase distribution h, we obtain the autocorrelation function of the spike train $L(t)$ as

$$L(t)=\int_0^{2\pi} h(\theta)l(t|\theta)d\theta. \tag{7}$$

For large t, the correlation between discharges decays and $L(t)$ tends to the T-periodic function $Q(t)$, given by

$$Q(t)=\frac{2\pi}{\langle t\rangle}\int_0^{2\pi} h([\theta+\Omega t])h(\theta)d\theta. \tag{8}$$

Thus, we can write $L(t)=R(t)+Q(t)$, with R decaying to zero for large t. Finally, the PSD of the discharge train, denoted by $P(\omega)$, is derived from L as [12]

$$P(\omega)=\frac{1}{\pi\langle t\rangle}(1+\tilde{L}(\omega)+\tilde{L}(-\omega))$$

$$=\frac{1}{\pi\langle t\rangle}\left(1+\tilde{R}(\omega)+\tilde{R}(-\omega)+2\pi\sum_n q_n\delta(\omega-n\Omega)\right), \tag{9}$$

where $\langle t\rangle$ is the mean ISI, $\tilde{L}$ and $\tilde{R}$ are defined as in Eq. (3), and the q_n are the coefficients of the Fourier expansion of Q, i.e.

$$q_n=\frac{1}{T}\int_0^T Q(t)e^{-in\Omega t}dt. \tag{10}$$

In this way, the SNR can be defined as

$$S=\frac{2\pi q_1}{1+\tilde{R}(\Omega)+\tilde{R}(-\Omega)}. \tag{11}$$

We also consider the following quantity which is the ratio between the area of the δ function in the PSD at the modulation frequency, and the base value at large frequencies (corresponding to the PSD of the Poisson impulse process with same mean ISI):

$$S^*=2\pi q_1. \tag{12}$$

One remarkable difference between the PSDs for endogenous [Eq. (2)] and exogenous [Eq. (9)] forcings is that the latter has peaks of infinite height at the modulation frequency and its harmonics, whereas the former has peaks of finite height near the modulation frequency. This difference stems from the fact that the autocorrelation function of the renewal process settles at a constant value, whereas for exogenous forcing it is asymptotically periodic. This periodicity reflects the correlation introduced by the stimulation. Because of the difference in the definitions of the SNRs, it is not possible to compare them quantitatively, however, it is possible to compare the optimal noise level that maximizes each of them and see whether they correspond.

SR-like behavior in the exogenously forced LIFM. As stated previously, the frequency domain analysis of the forced LIFM had been restricted to endogenous forcing [7,10] so that, in the first place, we examined whether SR-like behavior was also present for exogenous stimulation. Numerical computations [13] of the SNRs S and S^* for subthreshold inputs showed that both quantities are maximal at some intermediate noise intensities. The lower panels in Fig. 1 illustrate the humped shaped curves of noise versus S and S^*. Thus the presence of SR in the forced LIFM does not depend on the type of forcing. However, the SNRs for exogenous forcing reach their maxima at significantly larger noise intensities than for endogenous forcing. This difference results from the fact that endogenous forcing renders the system more sensitive to fluctuations, thus leading to a faster deterioration of the SNR with noise. Indeed, due to the resetting of the input phase at each discharge, noise induced variability in the discharge times translates into a decrease in the regularity of the input signal itself; in fact, the LIFM is forced by successive sequences of sinusoids, all starting at the same phase, but with variable length. As the noise is increased, so does the variability of the input sequence lengths and, consequently, the overall input departs from a periodic signal leading to a reduced regularity of the spike train.

Mean discharge frequency locking. The SR-like behavior in the LIFM with exogenous forcing occurs at noise levels that are close to time-scale matching. Therefore, the resetting of the input phase in the endogenously forced LIFM accounts in part for the lowering of the optimal noise level in comparison with the value predicted by time-scale matching. However, even for exogenous forcing, time-scale matching is not entirely satisfied. In the following, we show that another mechanism accounts for the enhanced response of the system.

Schematically, the response of the LIFM is enhanced through time-scale matching when its behavior in the presence of forcing is close to that with noise alone (without forcing). This is the case when, for example, the mean ISI with noise alone matches the modulation period, leading to a cooperative behavior between the two. For weak and slow subthreshold modulation, such effects account for the enhanced response of the system. However, for large subthreshold modulation, the forced noisy LIFMs are closer to systems undergoing suprathreshold forcing than to unmodulated systems. In this case, noise enhances the response of the system through a mechanism that differs from time-scale matching.

Essentially, noise renders possible firing in the presence of subthreshold forcing. In this sense, the effect of noise is to lower the system's threshold. This implies that a large subthreshold modulation acts effectively as a suprathreshold forcing when noise is increased. This in turn can lead to more regular discharges as suprathreshold forcing can evoke phase locked periodic discharges. In other words, the response of the LIFM to large exogenous subthreshold modulation can resemble noisy phase locked discharge trains for some range of intermediate noise intensities. This range is essentially determined by the distance between the input amplitude and the threshold rather than the characteristic time scales of the system in the absence of modulation.

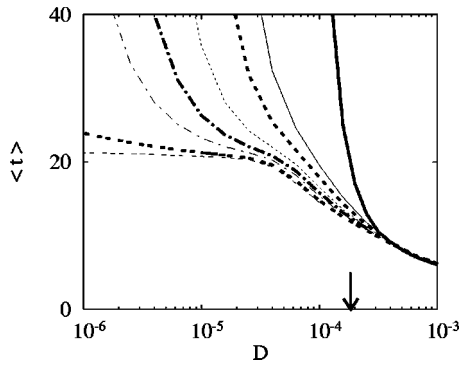

FIG. 2. Mean ISI $\langle t \rangle$ versus noise intensity D in $[(\mathrm{mV})^2/(\mathrm{ms})]$ for exogenous forcing. The lines show $\langle t \rangle$ for forcings with amplitudes $A=0$, 0.0225, 0.025, 0.0275, 0.029, 0.03, 0.0314, and 0.032 V/s from right to left. Only $A=0.032$ V/s is suprathreshold. The arrow indicates the noise intensity yielding $\langle t \rangle = T$ for $A=0$ (where T is the modulation period). Same parameters as in Fig. 1.

Figure 2 illustrates this phenomenon. Each line represents the evolution of the mean ISI of a forced LIFM for a given input amplitude as the noise is increased. The thick solid line is the mean ISI for ''spontaneous'' firing, i.e., without modulation. The thin dashed line below all others is for suprathreshold forcing. All other lines represent subthreshold forcings, with amplitudes increasing from right to left. As expected, for suprathreshold forcing, the mean ISI stabilizes at a finite value as the noise tends to zero, while the other curves tend to infinity. At large noise levels, all curves merge into one, indicating that in this regime, the input plays little role in determining the response of the system; the firing is noise dominated. For the intermediate range of noise, the mean ISIs for subthreshold forcings take on two forms. For low amplitudes ($A=0.0225$ and 0.025), they decay rapidly much in the same way as for $A=0$. As the amplitude is increased, the curves present an inflection: first they approach the mean ISI for suprathreshold forcing, and then they decay along this curve. The larger the input amplitude is, the more pronounced this phenomenon appears. Indeed, for large enough subthreshold modulation, the mean ISI displays a plateaulike flattening in the intermediate range of noise. In this regime, the LIFM fires with a mean ISI close to the modulation period T. Furthermore, the ISIs are close to T, and the phase distribution displays a marked peak; the firing is almost one to one phase locked [6,14]. We refer to this regime as mean discharge frequency locking. It is in this range of noise, where the LIFM behaves like a noisy system forced by a suprathreshold modulation, that the SNR reaches its maximal value.

Besides illustrating the mechanisms that lead to an enhanced response, the curves in Fig. 2 also clarify the difference between mean discharge frequency locking and time-scale matching as well as mean switching frequency locking in threshold devices. In time-scale matching, the response of the system is near optimal when, say, the mean ISI of the unforced system equals the modulation period [6]. Similarly, mean switching frequency locking occurs when the mean interthreshold-crossing intervals approach the modulation period [8]. However, in contrast to these results, (i) the flattened plateaus in Fig. 2 occur for noise levels that are significantly below the one that yields a mean ISI equal to the

modulation period in the unforced system (indicated by the arrow in the figure) and (ii) both the lower and higher ends of the plateaus shift progressively to lower noise levels as the signal amplitude approaches the threshold. These two characteristics further confirm that the mean discharge frequency locking and the resulting enhanced response of the LIFM are consequences of the proximity of the threshold rather than matching between the mean ISI of the unforced system and the modulation period.

The responses of the deterministic LIFM to sinusoidal input are phase locking or quasiperiodic behavior. In the A-T parameter plane, phase locking regions form characteristic bands, referred to as Arnold tongues. Their structure has been studied in [11]. To analyze the correspondence between the mean discharge frequency locking (of the stochastic model) and the Arnold tongue structure (for the deterministic system), we have computed the average number of firings per cycle, and examined its dependence on A, T, and the noise intensity. In the absence of noise, the three-dimensional plots of the averaged number of firings per cycle against A and T display a staircaselike shape with flat steps corresponding to phase locking regions (not shown). The addition of noise and progressive increase of its intensity smooths the staircaselike structure and, eventually, for large noise, the structure is changed into a slope without flat plateaus. Another effect of noise is to lower the boundaries of phase locking regions [15]. For the parameter set in Fig. 2, the lower boundary of the 1:1 locking region is close to the threshold. With the addition of noise, this boundary progressively moves into the subthreshold region before the 1:1 locking plateau disappears, thus leading to the mean discharge frequency locking as was observed in Fig. 2.

In conclusion, our analysis of the response of the noisy LIFM to large subthreshold modulation is hinged upon the derivation of an expression for the PSD and the SNR of this system. Using these quantities we showed that this system, similarly to endogenously forced LIFMs, displays SR-like behavior. Finally we characterized the enhanced response of the system in terms of mean frequency locking appearing for large subthreshold signals rather than time-scale matching.

[1] J.K. Douglass *et al.*, Nature (London) **365**, 337 (1993); J.E. Levin and J.P. Miller, *ibid.* **380**, 165 (1996); X. Pei and F. Moss, J. Neurophysiol. **76**, 3002 (1996); J.J. Collins, T.T. Imhoff, and P. Grigg, *ibid.* **76**, 642 (1996).

[2] A. Longtin, A.R. Bulsara, and F. Moss, Phys. Rev. Lett. **67**, 656 (1991); A. Longtin, J. Stat. Phys. **70**, 309 (1993); X. Pei, K. Bachman, and F. Moss, Phys. Lett. A **206** 61 (1995); J.J. Collins, C.C. Chow, and T.T. Imhoff, Nature (London) **376**, 236 (1995); D.R. Chialvo, A. Longtin, and J. Müller-Gerking, Phys. Rev. E **55**, 1798 (1997); A. Capurro *et al.*, *ibid.* **58**, 4820 (1998).

[3] F. Moss, D. Pierson, and D. O'Gorman, Int. J. Bifurcation Chaos Appl. Sci. Eng. **4**, 1383 (1994); A.R. Bulsara and L. Gammaitoni, Phys. Today **49** (3), 39 (1996); L. Gammaitoni *et al.*, Rev. Mod. Phys. **70**, 223 (1998); K. Wiesenfeld and F. Jaramillo, Chaos **8**, 539 (1998).

[4] A.R. Bulsara, S.B. Lowen, and C.D. Rees, Phys. Rev. E **49**, 4989 (1994).

[5] A.R. Bulsara *et al.*, Phys. Rev. E **53**, 3958 (1996).

[6] A. Longtin and D.R. Chialvo, Phys. Rev. Lett. **81**, 4012 (1998).

[7] T. Shimokawa, K. Pakdaman, and S. Sato, Phys. Rev. E **59**, 3427 (1999).

[8] B. Shulgin, A. Neiman, and V. Anishchenko, Phys. Rev. Lett. **75**, 4157 (1995).

[9] P. Lánský, Phys. Rev. E **55**, 2040 (1997).

[10] H.E. Plesser and S. Tanaka, Phys. Lett. A **225**, 228 (1997).

[11] J.P. Keener, F.C. Hoppensteadt, and J. Rinzel, SIAM (Soc. Ind. Appl. Math.) J. Appl. Math. **41**, 503 (1981); T. Tateno, J. Stat. Phys. **92**, 675 (1998); S. Coombes and P. Bressloff, Phys. Rev. E (to be published).

[12] M.S. Bartlett, *An Introduction to Stochastic Processes* (Cambridge University Press, Cambridge, New York, 1966).

[13] As shown by Eqs. (5–8), the two functions L and Q can be computed from the conditional density g and the phase distribution h. The function R can then be computed as $L-Q$. Thus all quantities necessary for the evaluation of S and S^1 can be computed using the method in [7]. Examples of the comparison of the results from this approach and those obtained from numerical resolution of the stochastic differential equation (1) have yielded satisfactory results and will be presented in T. Shimokawa *et al.* (unpublished).

[14] T. Tateno *et al.*, J. Stat. Phys. **78**, 917 (1995).

[15] A simillar phenomenon has been reported by Longtin for the FitzHugh-Nagumo model; see A. Longtin, Chaos Solitions Fractals (to be published).